A simplified approach to numerical modelling of an underground pumped hydroelectric energy storage system

G. Zamani[1], A. Franza[1], K.K. Sørensen[1], L.V. Andersen[1], S. Tourchi[2], H.H. Stutz[3]

[1] Dept. of Civil and Architectural Engineering, Aarhus University, Aarhus, Denmark
[2] Faculty of Science, Charles University, Prague, Czech Republic
[3]Institute of Soil Mechanics and Rock Mechanics, Karlsruhe Institute of Technology, Karlsruhe, Germany

ABSTRACT: The Underground Pumped Hydroelectric Storage (UPHS) is an energy storage system in which inflation and deflation of an underground geomembrane–lined reservoir interconnected to an open water basin enable the storing and harvesting of energy, respectively, in terms of potential energy. Axisymmetric Finite-Element Analyses (FEA), including monotonic and multi-cycle changes of the reservoir volume, are used to investigate reservoir aspects that influence the capacity and efficiency of UPHS in sand, including geomembrane stiffness and interface friction. In particular, a novel simplified approach for the modelling of UPHS reservoir is proposed. This consists of rigid piston elements lifting within a skirt incompressible material with low shear stiffness and directly tied to the overburden. The simplified approach is validated against refined models having the reservoir as a lined fluid cavity undergoing volume changes. Results indicated that the simplified modelling is suitable for preliminary estimates of overburden deformations, reservoir pressure–volume curves, and energy efficiency. Also, practical design guidelines are suggested that can help engineers to design resilient UPHS systems.

Keywords: Finite Element; Modelling; Energy Storage; Buried Reservoir; Overburden.

1 INTRODUCTION

The increase in the share of renewable energy is a challenge for the green transition due to the intermittency of renewable sources such as wind. To store surplus renewable energy from intermittent sources, energy storage is required that can improve the stability and efficiency of the electricity supply. Among other systems, the Underground Pumped Hydroelectric Storage (UPHS) can be used: potential energy is stored by inflating an impermeable geomembrane-lined bag buried underneath a manmade overburden with water from a nearby basin; energy is recovered by discharging the pressurised water towards the basin across a pipeline connected to a turbine (Olsen et al., 2015). A reduced-scale (1:10) field trial of the full-size UPHS system with an initial reverse configuration, as schematically shown in Figure 1, has been conducted at Aarhus University in Foulum, Denmark (Franza et al., 2022).

Despite preliminary works, numerical simulations (Norlyk et al. 2020), small-scale physical modelling (Sørensen et al. 2022) and measurements from field trials (Franza et al. 2022) indicated that geometrical, mechanical, and operational parameters (such as, overburden geometry, soil behaviour, maximum inflation volume) may affect UPHS performance per cycle. In particular, the design of UPHS system poses two main geotechnical challenges: (i) predicting the accumulated overburden deformations, (ii) estimating

the energy losses within the system constituted by the reservoir and overburden induced at element level from material irreversible deformations and frictional losses. Norlyk et al. (2020) illustrated an accumulation of outward movements of the central overburden that leads to a cover reduction after less than 25 cycles, which is a relatively small number. To estimate (ii), the difference between the input E_I and discharged E_d stored energies can be calculated by integrating the pressure p at the reservoir inlet with respect to the volume from the initial V_I to the final volume V_f and vice versa, respectively, giving an energy loss ΔE and an efficiency $\eta = E_d/E_I$ for a given cycle.
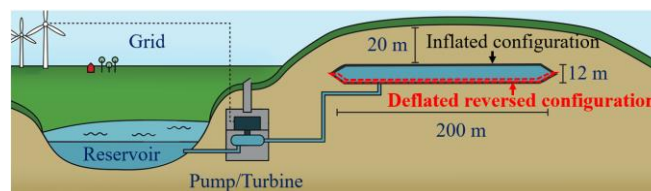

Figure 1. Principle of reversed geomembrane–lined bag for UPHS at prototype scale (Franza et al., 2022).

This paper presents axisymmetric Finite Element Analyses (FEA) to investigate the response of UPHS systems in dry sand with an initial reverse configuration and a hill-shaped overburden. The influence of the overburden geometry, the reservoir bag stiffness, and the frictional contact between the overburden and the

reservoir on the efficiency, η, the reduction in overburden cover, and the shape of the overburden surface over multi-cycle operations are examined. Furthermore, two modelling approaches for the modelling of the reservoir are compared to identify viable modelling strategies for preliminary design, namely: a Lined Fluid Cavity Reservoir (LFCR) consisting of a fluid cavity subjected to a volume change within a buried geomembrane-lined bag interacting with the reservoir through a frictional interface; and a Piston Displaced Incompressible Reservoir (PDIR) consisting of rigid elements lifting within a skirt of incompressible material with low shear stiffness and directly tied to the overburden. Finally, practical aspects of UPHS design inferred from the numerical results are discussed.

2 NUMERICAL MODELLING

2.1 Studied UPHS configuration

As shown in Figure 2, all axisymmetric simulations modelled a reduced-scale (1:10) UPHS system with hill-shaped configuration: overburden cover $C = 4$ m from the reservoir upper membrane, height $T = 2$ m above the original ground level, offset from the reservoir edge $O = 2$ m, and external slope 26.6° (slope 1:2); the initial reversed configuration of the reservoir has side length $L = 20$ m, depth $D = 1.2$ m, and side slopes of 26.6° (slope 1:2). Thus, the *nominal lift height* is $U_\text{n} = 2D = 2.4$ m, whereas the *nominal fully inflated volume* is $V_\text{n} = 594.7$ m³ for the ideal reversed shape.

The geomembrane has a thickness of 2.0 mm and a Young's modulus of 90 MPa, similarly to that of polypropylene-polyethylene GSE ProFlex. For the overburden, a dry sand is considered with a friction angle of $\varphi = 37°$, a cohesion of 5 kPa, a Young's modulus of 10.9 MPa, a Poisson's ratio of 0.33, a dilation angle of 2°, a dry unit weight of $\gamma = 17$ kN/m³, and a lateral earth pressure coefficient of $K_0 = 0.41$. The membrane–overburden friction angle is assumed to be $\delta = 5.7°$ if not stated otherwise, providing a friction coefficient of $\mu = \tan(5.7°) = 0.1$. To describe the overburden uplift due to changes in the reservoir volume, the *average lift* is defined as $U_\text{avg} = R_v U_\text{n}$ that relates the nominal uplift U_n to the volume ratio $R_V = V/V_\text{n}$, where V is the reservoir water volume.

In this paper, three types of UPHS operations are investigated: monotonic inflation up to $U_\text{avg}/L = 7\%$ that corresponds to $R_v = 58.3\%$; single- and multi-cycle (7 cycles) analyses for average uplift-to-side length ratio U_avg/L between 1.3% to 3.8% corresponding to R_V between 5% and 35%, respectively.

2.2 Numerical approaches to model the reservoir

To predict UPHS mechanical behaviour over multi-cycle analyses, refined LFCR and simplified PDIR axisymmetric FEA of the boundary value problems were developed using Simulia ABAQUS (2021) and Optum G2 (2021) 2.1.6, respectively. A view of the PDIR is shown in Figure 2, while deformed shapes and meshes are shown for the inflated state of cycle 1 in Figure 3 for both models. A Mohr-Coulomb constitutive model with a non–associated flow rule is assumed for the overburden. The greatest difference is the approach used to simulate the underground reservoir and the geomembrane-lined bag, as described in the following.

The refined Abaqus model explicitly models the LFCR: the upper and lower geomembranes are simulated using linear elastic shell elements (*SAX1*); the bottom layer is modelled as linear elastic with perfect fixities as boundary conditions. The upper membrane is in equilibrium with the overburden and a reservoir pressure; a surface-to-surface contact with a frictional interface. The penalty method is applied for tangential behaviour and the normal behaviour is modelled using augmented Lagrange method. Hard contact is adopted between the membrane and the overburden (*CAX4* elements) using the mortar method in which the overburden and top membrane segments are set as secondary and main, respectively; a similar contact is prescribed between the upper and lower membranes to capture potential local contact of the reservoir bag at the deflated state; incompressible fluid cavity elements connect the reservoir to a nearby basin to model changes in the reservoir volume V. This approach has been previously adopted from Norlyk et al. (2020) and Stutz et al. (2020); despite this, convergence difficulties occurred when developing the LFCR models, indicating the LFCR's shortcomings for sensitivity studies. To facilitate convergence, an elastic region with Young's modulus of the soil is assigned to the overburden region at the reservoir edge, as shown in Figure 3(b). In the LFCR model, the reservoir is set to an initial volume $V = 69.37$ m³ giving an initial $U_\text{avg}/L = 1.4\%$.

The Optum G2 model simplifies the water-filled bag subjected to volume changes to a PDIR, with no explicit modelling of the geomembrane-lined bag. The reservoir consists of incompressible solid with negligible shear stiffness and having the unit weight of water: it is laterally confined within a vertical rigid skirt perfectly fixed and with a small gap to the piston; it is directly tied at the top to the overburden; it is displaced at its bottom by a rigid plate of U_piston so that $V = U_\text{piston} \pi L^2/4$ (i.e., the piston simulates the change in volume of the reservoir by upward and downward movements, with $U_\text{piston} \approx 1.27 R_v V_\text{n}/L^2$ differing from $U_\text{avg} = R_v U_\text{n}$). PDIR assumes the upper membrane layer as fully flexible and bounded by a rough interface to overburden bottom surface with no possible slippage. For the incompressible material, the reservoir, a frictionless Mohr–Coulomb constitutive model with associated flow rule is assumed with a large bulk modulus of 2 200 MPa, a low shear stiffness of 10 kPa, and a relatively small

cohesion of 10 Pa. For both the overburden and the incompressible solids, *6-node Gauss* triangular elements available in Optum G2 are adopted, having quadratic interpolation of displacements and linear interpolation of stresses (with stress points at the Gauss points). This approach is proposed for the first time, to the authors' knowledge, to bypass the modelling of a complex boundary problem at early design stages of UPHS systems.
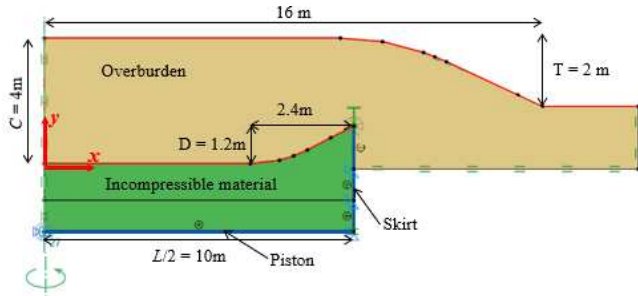

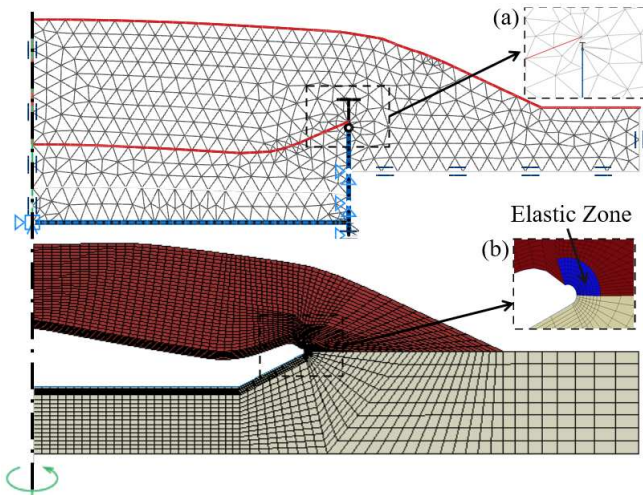*Figure 2. FEA model for "Piston displaced incompressible reservoir".*

Figure 3. Mesh and deformed shape of (a) PDIR and (b) LFCR model at cycle 1 inflation.

Both models assume a constant pressure throughout the reservoir (i.e., no pressure gradient with the reservoir due to the water density). This reservoir pressure P^* is equal to the "overburden pressure" (i.e., a reaction of the water on the overburden), it is the result of the mass of the overburden as well as the overburden's internal strength and stiffness. In the Abaqus model, the effects of geometric nonlinearities (due to large displacements and changes in overburden shape) are accounted for, whereas they are neglected in the Optum G2 model; this aspect is later discussed.

Note that a geostatic analysis step is needed for the overburden to reach equilibrium with the reservoir before inflations. The resulting reservoir pressure from the geostatic step is $P_0^* = 0.91\gamma C$, as average of PDIR and LFCR models, due to overburden arching at the reservoir sides.

2.3 Comparison of single–cycle and monotonic inflation analyses

To validate simplified PDIR predictions with respect to LFCR, Figure 4 shows for both types of models monotonic inflation and single-cycle results in terms of normalised reservoir pressure $P^*/\gamma C$ (initial values are approximately $P_0^*/\gamma C = 0.91$), membrane strain (negative values being compressive) as well as percentage cover variation at the centre locations for $x = 0$ (negative values associated with cover reduction). To allow a direct comparison, the initial piston position is associated with $U_{\mathrm{avg}}/L = 1.4\%$ to accommodate the fact that the LFCR model has an initial volume $V = 69.37$ m^3 (e.g., the PDIR results in Figure 4 are offset by 1.4% on the abscissa). Additionally, to compare the LFCR and the PDIR predictions at large uplift values, monotonic inflation analyses were carried out to identify the upper limit of the reservoir inflation volume (when defining performance thresholds as membrane strains and cover reduction) while the single-cycle results provide insights into the system response during deflation.
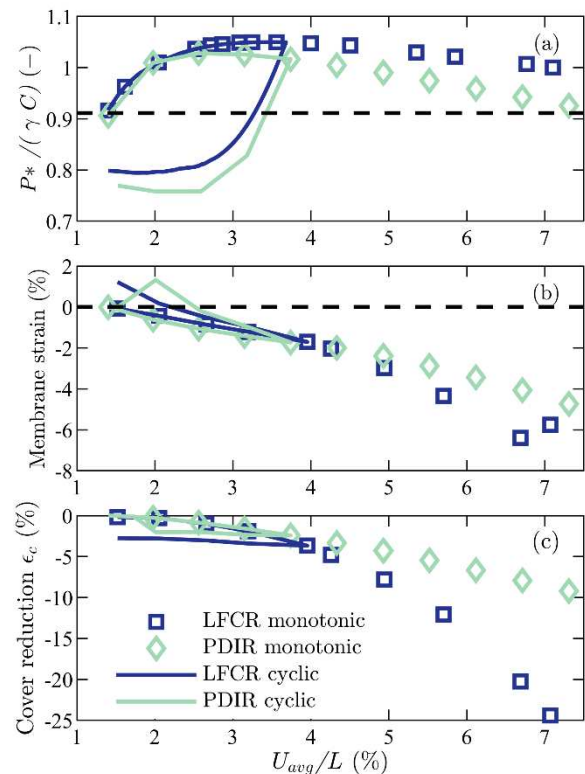

Figure 4. Monotonic and single–cycle analyses: (a) reservoir pressure; membrane strain (b) and cover reduction (c) at the centre.

Monotonic analyses in Figure 4(a) show a softening trend in reservoir pressure P^* during the reservoir inflation: namely, P^* displays an initial increase from P_0^* up to a peak value of $1.028\gamma C$ and $1.05\gamma C$ for the PDIR and LFCR, respectively, at an uplift U_{avg}/L within 2.6%–2.8% for both models; this is followed by a steady

reduction for further inflation. Interestingly, despite similar trends, the P^* values predicted by the PDIR and LFCR models are not identical. Small uplift values tend to diverge the following peak levels with the PDIR model overestimating softening, possibly due to geometrical nonlinearities being considered in the LFCR model. Consider that the equilibrium of the overburden soil mass and shear reaction stresses to the imposed overburden deformation by the reservoir volume change results in P^*. Thus, the increase in P^* at small uplift is the result of the overburden shear strength and stiffness, whereas the softening response may be due to overburden arching towards the reservoir edges. Importantly, single-cycle results from the PDIR and LFCR models are in good agreement, with P^* displaying a hysteretic trend when plotted against the average uplift U_{avg}/L that is associated with energy losses.

Next, membrane and overburden deformations are considered. Monotonic inflation induces compressive membrane strains only (see Figure 4(b)) with comparable values predicted by both models, which is induced by (i) the friction mobilised with the overburden, (ii) the membrane behaving as a flexible body (as later discussed), and (iii) the overburden lower part being subjected to horizontal compressive stresses and strains (similarly to an unreinforced simply supported beam subjected to uniform loading); this compressive mechanism does not pose a thread for mechanical distress of the membrane. Contrarily, during the deflation of cycle 1 the membrane strain reaches tensile values. Therefore, tensile membrane deformations should be assessed in multi-cycle simulations.

Figure 4(c) shows cover reduction at the central axis of $\varepsilon_{\mathrm{c}} \approx -3\%$ for the operational maximum inflation uplift $U_{\mathrm{avg}}/L = 3.8\%$ in the PDIR and LFCR models. More importantly, monotonic LFCR results above U_{avg}/L of 5% (above peak reservoir pressure P_{max}^* when the reservoir pressure has a steep softening) are characterised by a steep increase in the cover reduction per unit uplift (i.e., the slope of the curves in Figure 4(c)). Considering that the cover reduction induced by the inflation single cycle does not recover during deflation, this indicates that (i) cover reduction is induced by irreversible strains of the elastoplastic material and (ii) that there is the risk for its accumulation for multi-cycle analyses (thus investigated by multi-cycle analyses).

It is of interest to compare overburden surface displacements with upper membrane displacement for the two models. Figure 5 shows monotonic inflation results at $U_{\mathrm{avg}}/L = 3.8\%$ and 7%, with the former value corresponding to cycle 1, inflated state. The PDIR position profiles nearly match the LFCR results (see subplots (a) and (b)); contrarily, small differences in central uplift of the reservoir occur above peak pressure

P^* for U_{avg}/L of 7.0% (see subplot (d)). Thus, P_{max}^* from monotonic inflation analyses (simple to compute) can be used to identify the upper limit of the applicability of PDIR models.
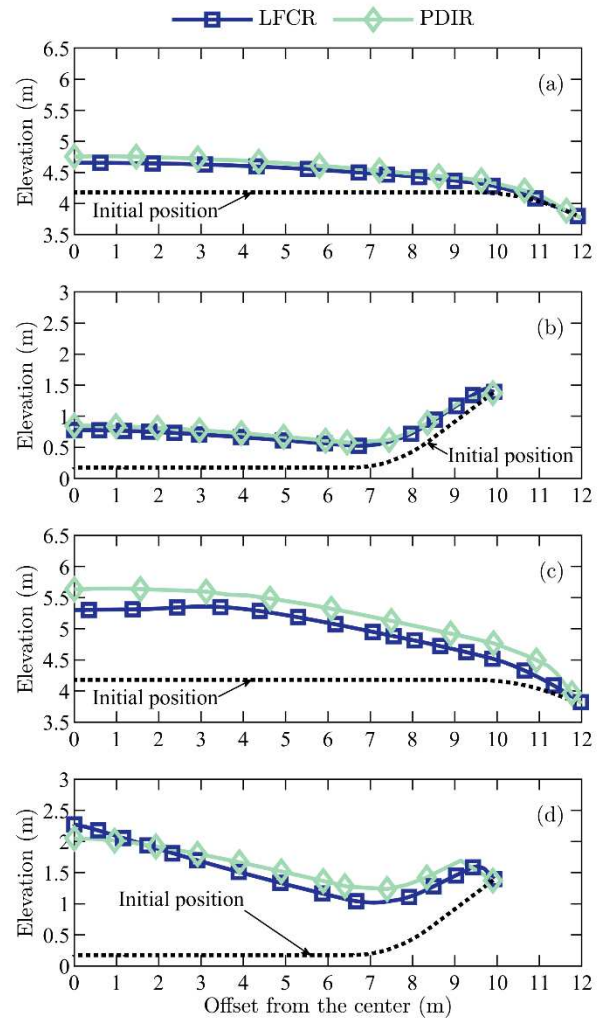

Figure 5. Displacement results for monotonic inflation: (a, c) soil surface and (b, d) upper membrane profiles for $U_{avg}/L=$ 3.8% (a, b) and 7% (c, d).

Figure 6 shows a sensitivity study regarding the effects of the membrane-to-soil friction coefficient μ on the overburden movements and upper membrane meridional strains. The study is done by monotonic LFCR analyses for $U_{\mathrm{avg}}/L = 3.8\%$. Additionally, PDIR outcomes are reported in this figure to evaluate the fidelity of the PDIR's assumptions of the upper membrane perfectly tied to the overburden. Overall, while the influence of the interface friction coefficient μ on the UPHS geo–structure displacements is minimal (for the overburden surface as well as the reservoir), it controls the upper membrane strain profile. There is a good agreement between PDIR and LFCR for a perfectly rough interface ($\mu = 1$, thus $\delta > \varphi$). More importantly, the LFCR outcomes are nearly identical for $\mu = 0.1$ and 1, corresponding to a low interface friction angle, $\delta = 5.7°$, and a perfectly rough interface, $\delta > \varphi$, respectively. Hence, the PDIR assumptions of an upper

membrane tied to the soil are applicable even if the interface friction angle δ is significantly lower than soil internal friction angle φ. On the other hand, the results indicate larger compressive strains in the central part of the membrane for a (nearly) smooth interface, due to the lack of compatibility between the overburden and the relatively flexible membrane.
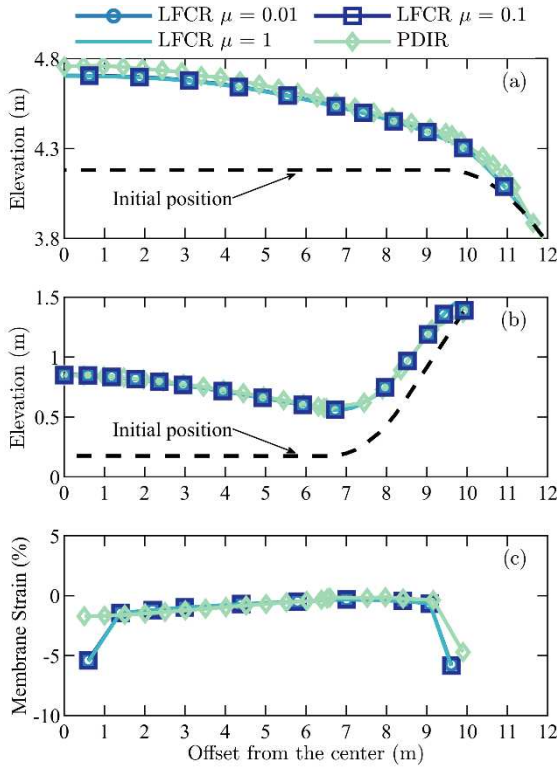

Figure 6. Influence of interface friction coefficient on monotonic results at U_{avg}/L =3.8%: (a) soil surface; (b) upper membrane profiles, (c) membrane strain.

Finally, the influence of the membrane stiffness is studied. LFCR monotonic analyses carried out for membrane Young's moduli of 9 to 90 MPa; results indicated nearly identical displacement and strain profiles of the UPHS. Therefore, if the reservoir bag has an axial stiffness (i.e., product of geomembrane thickness and Young's modulus) of 180 kN/m, it behaves as a fully flexible impermeable layer.

2.4 Results for multi-cycle analyses

Despite the adopted linear elastic–perfectly plastic Mohr–Coulomb constitutive model for the overburden, the PDIR and LFCR models were run and compared for a total of 7 cycles for a dual scope: primarily to compare the two modelling techniques under a relevant type of boundary condition; secondarily, to identify possible behaviours of the UPHS system.

Figure 7 displays single- and multi-cycle reservoir P^* variations with normalised average uplift. As previously indicated, there is an overall agreement between the two models, with cycle 1 slightly differing from cycles 2–7

because, when deflating down to U_{avg}/L = 1.3%, the reservoir pressure is lower than the initial value P_0^*. Based on Figure 7, the average energy efficiency of the UPHS system is estimated to be η = 82.7% and 84.7% for the PDIR and LFCR, respectively, with almost no variation between cycles.
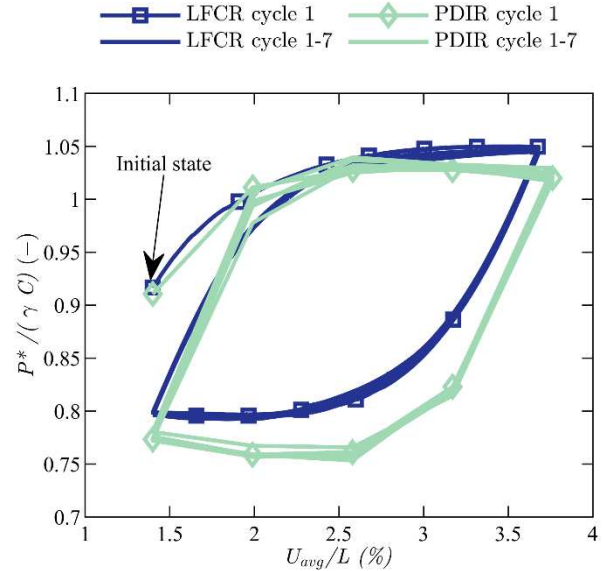

Figure 7. Reservoir pressure against average uplift in multi-cycle analyses.

Finally, UPHS displacements and deformations at the inflated state of cycles 1 and 7 are compared in Figure 8 for both modelling techniques. Figures 8(a) and (b) indicate a reduction in the central uplift of the system (both surface and reservoir) associated with outward movement of the overburden side and cover reduction. Although the two models do not perfectly match at cycle 7, the deformation mechanisms predicted by the PDIR and LFCR models are qualitatively in agreement. The cover reduction at the inflated state at cycle 7 increased during operations to $\varepsilon_c = -9\%$ and -6% for the PDIR and LFCR models, respectively, with the PDIR model providing a conservative estimate. Furthermore, both models indicate a relatively large tensile straining of the membrane at the central area up to an offset of 2 m from the centre in Figure 8(c), indicating a risk of membrane damage if compared with a linear elastic regime of 5% biaxial tensile straining of the geomembrane used in the field trial by Franza et al. (2022); as for the elevation profiles, the membrane strains inferred from the PDIR and LFCR models are in qualitative agreement with the PDIR model providing a conservative assessment, possibly due to assuming a perfectly rough interface.
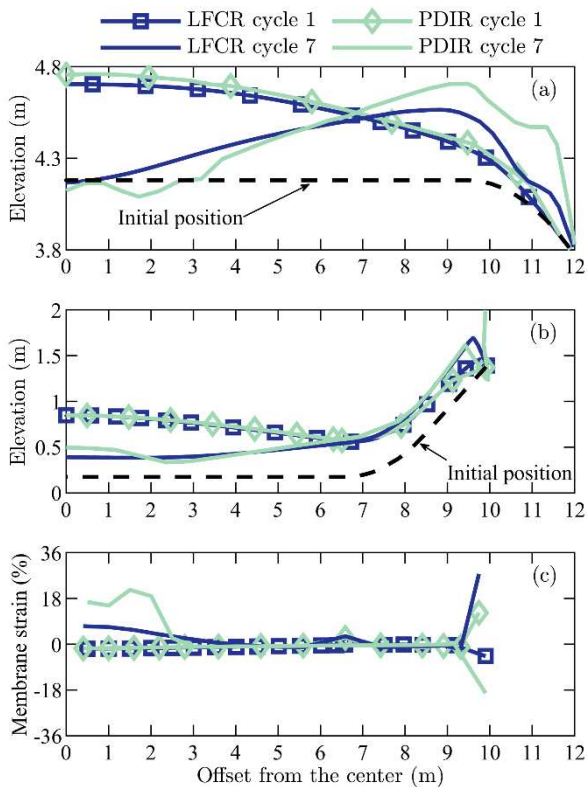
Figure 8. Multi-cycle results: (a) soil surface; (b) upper membrane profile; (c) membrane strain.

3 CONCLUSIONS

This paper studies the response of reduced scale (1:10) UPHS systems in dry sand with an initial reverse configuration and a hill-shaped overburden.

A novel simplified approach for the modelling of the buried geomembrane-lined reservoir is proposed, named Piston Displaced Incompressible Reservoir, which is validated against refined fluid cavity results. When adopting a Mohr–Coulomb constitutive model for the sandy overburden, the proposed modelling approach is in good agreement with the refined outcomes for both monotonic inflation (up to large uplift associated with cover reduction of 2%) and multi-cycle with an average uplift of 19% the cover height (leading to variation in the reservoir inflation and overburden deformations compared with single-cycle analyses). Results indicated that the simplified modelling is suitable for quick estimates of overburden deformations, reservoir pressure–volume curves, and energy efficiency. The following practical conclusions for the design of UPHS in sand are drawn.

• Overburden reaction stresses may be characterised by softening during inflation, which has implications for the energy storage per unit uplift.

• The considered geomembrane behaved as a fully flexible impermeable layer. The interface friction angle between geomembrane and overburden controlled the tensile strains in the membrane, but it did not impact the UPHS displacement being the membrane relatively flexible. To assume that the upper geomembrane is a fully flexible membrane, tied to the overburden, is reasonable as long as the friction coefficient μ of the interface between membrane and soil is equal to or greater than $0.1 \tan \varphi$. Sensitivity studies on μ are recommended for design.

• Multi-cycle operations reaching a maximum inflation volume above the peak reservoir pressure indicated that irreversible (plastic) strains of the overburden accumulate with each cycle leading to a central cover reduction, outwards moment of the overburden, and membrane tensile strains. Monotonic analyses may identify operational reservoir inflation volume for performance thresholds as percentage cover reduction; contrarily, multi-cycle simulations are recommended for the estimation of tensile membrane strains.

Future works will study, for varying soil type, the effect of overburden initial geometry at full prototype scales. Also, advanced constitutive models capturing nonlinear soil behaviour will be used.

4 ACKNOWLEDGMENTS

5 REFERENCES

Franza, A., Sorensen, K.K., Stutz, H.H., Pettey, A., Heron, C., Marshall, A.M. 2022. Field and centrifuge modelling of a pumped underground hydroelectric energy storage system in sand. *Proceedings, 10th International Conference on Physical Modelling in Geotechnics*, 754–757. Seoul, South Korea.

Norlyk, P., Sørensen, K., Andersen, L.V., Sørensen, K.K., Stutz, H.H. 2020. Holistic simulation of a subsurface inflatable geotechnical energy storage system using fluid cavity elements, *Computers and Geotechnics* **127**, 103722.

Olsen, J., Paasch, K., Lassen, B., Veje, C.T. 2015. A new principle for underground pumped hydroelectric storage, *Journal of Energy Storage* **2**, 54–63.

Sørensen, K.K., Stutz, H., Brødsgaard-Raptis, P., Luxhøj, M. 2021. Conceptual physical modelling of a subsurface geomembrane energy storage system. *Proceedings, 20th International Conference on Soil Mechanics and Geotechnical Engineering*. Sydney, Australia.

Stutz, H.H., Norlyk, P., Sørensen, K, Andersen, L.A., Sørensen, K.K., Clausen, J. 2020. Finite element modelling of an energy–geomembrane underground pumped hydroelectric energy storage system. *Proceedings, 2nd International Conference on Energy Geotechnics*, 07001. San Diego, California, USA.